

Benzofuran-fused Phosphole: Synthesis, Electronic, and Electroluminescence Properties

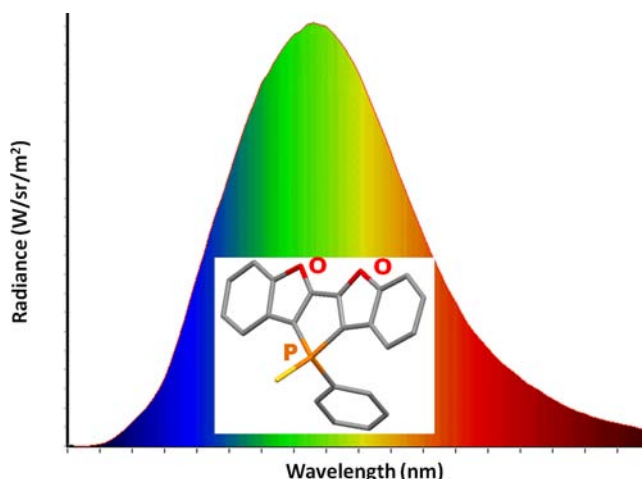
Hui Chen,[†] Wylliam Delaunay,[‡] Jing Li,[†] Zuoyong Wang,[†] Pierre-Antoine Bouit,[‡] Denis Tondelier,[§] Bernard Geffroy,^{||} François Mathey,^{†,⊥} Zheng Duan,^{*†} Régis Réau,^{*‡} and Muriel Hissler^{*‡}

International Phosphorus Laboratory, College of Chemistry and Molecular Engineering, Zhengzhou University, Zhengzhou 450001, P. R. China, Institut des Sciences Chimiques de Rennes, CNRS - Université de Rennes 1, Campus de Beaulieu, 35042 Rennes, France, Laboratoire de Physique des Interfaces et Couches Minces, CNRS UMR 7647, Ecole Polytechnique, 91128 Palaiseau, France, Laboratoire de Chimie des Surfaces et Interfaces, CEA Saclay, IRAMIS, SPCSI, 91191 Gif-sur-Yvette, France, and Nanyang Technological University, CBC-SPMS, 21 Nanyang Link, Singapore 637371, Singapore

*regis.reau@univ-rennes1.fr, muriel.hissler@univ-rennes1.fr, duanzheng@zzu.edu.cn

Received November 27, 2012

ABSTRACT



A synthetic route to novel benzofuran-fused phosphole derivatives 3–5 is described. These compounds showed optical and electrochemical properties that differ from their benzothiophene analog. Preliminary results show that 4 can be used as an emitter in OLEDs, illustrating the potential of these new compounds for opto-electronic applications.

π -Conjugated organic systems are highly versatile materials for the development of efficient electronic devices.¹ In particular, a great variety of S-containing π -conjugated

derivatives based on the thiophene scaffold have proven to be very efficient semiconducting materials for opto-electronic devices (Organic Light Emitting Diodes (OLED), Organic Solar Cells (OSC), and Field Effect Transistors (OFET)).² In the last years, other heteroles appeared as

[†] Zhengzhou University.

[‡] CNRS - Université de Rennes 1.

[§] Ecole Polytechnique.

^{||} CEA Saclay.

[⊥] Nanyang Technological University.

(1) (a) Müllen, K.; Scherf, U., Eds. *Organic Light Emitting Devices: Synthesis Properties and Applications*; Wiley-VCH: Weinheim, Germany, 2006. (b) Cheng, Y.-J.; Yang, S.-H.; Hsu, C.-S. *Chem. Rev.* **2009**, *109*, 5868. (c) Usta, H.; Facchetti, A.; Marks, T. J. *Acc. Chem. Res.* **2011**, *44*, 501.

(2) (a) Roncali, J. *Chem. Rev.* **1997**, *97*, 173. (b) Mishra, A.; Ma, C.-Q.; Bäuerle, P. *Chem. Rev.* **2009**, *109*, 1141. For specific reviews on OSC, OFET and OLEDs, see: (c) Thomson, B. C.; Fréchet, J. M. J. *Angew. Chem., Int. Ed.* **2008**, *47*, 58. (d) Allard, S.; Forster, M.; Souharce, B.; Thiem, H.; Scherf, U. *Angew. Chem., Int. Ed.* **2008**, *47*, 4070. (e) Gather, M. C.; Köhnen, A.; Meerholz, K. *Adv. Mater.* **2011**, *23*, 233.

appealing building blocks for the tailoring of conjugated materials since they possess electronic properties that markedly differ from those of thiophene. For example, the aromatic character of furan and phosphole is less pronounced than in thiophene, resulting in an increased exocyclic conjugation ability of their π -systems.³ However, this less pronounced aromatic character also confers to these heteroles a lower stability which can be circumvented by performing appropriate structural modifications on these heteroles. Stable furan-containing π -systems **A** and α -oligofurans⁴ **B** showing promising results as an active layer in organic/hybrid solar cells and OFETs have been described very recently.⁵ Likewise, the use of phosphole scaffolds for constructing organic materials **A–C** (Figure 1) has started in the past decade.⁶ In these materials, exploiting the reactivity and coordination chemistry of the reactive P-centers allowed controlling both their HOMO–LUMO gap and solid-state organization.⁷ Indeed, this unique molecular engineering afforded conjugated P-derivatives that can be used as advanced materials in OLEDs, including white-emitting devices or for the development of fibers, gels and liquid crystals.⁸ Derivatives of type **A** or **C** associating phosphole and thiophene moieties have been widely investigated.⁶ In contrast, mixed phosphole–furan compounds

are quite rare. Only linear systems **A** are known to date, and these compounds display a moderate emission property, precluding their use in optoelectronic devices.⁹ Therefore, we have been interested in P,O-based acenes associating phosphole and furan rings since structure rigidification generally improves the emission properties of π -conjugated organic systems.

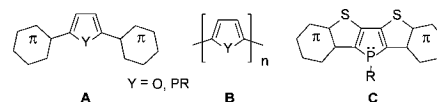
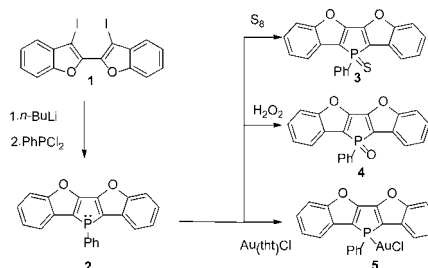


Figure 1. Phosphole-based π -conjugated systems **A**, **B** and **C**.

In this paper, we describe the synthesis, structure, and electronic properties of the first mixed phosphole–furan acene **2** (Scheme 1). Proper derivatization of this scaffold using the reactivity of the $\sigma^3\lambda^3$ -P center afforded compounds exhibiting good thermal stability and high emission quantum yields. These appealing properties have been exploited for the fabrication of OLEDs.

To design stable mixed furan–phosphole π -systems, the fused heteroacenic structure **2** (Scheme 1) was targeted since the benzofuran moiety exhibits a good stability due to the annelation of the two aromatic rings. The target compound **2** was synthesized by using a modified synthetic procedure reported by Baumgartner et al. for the preparation of mixed thiophene–phosphole heteroacenes **C** (Figure 1).^{6b,7f} The iodo-substituted benzofuran **1** was subsequently treated with 2 equivalents of *n*-BuLi and one equivalent of PhPCl_2 at -78°C affording compound **2** (^{31}P NMR: -44.0 ppm). Since $\sigma^3\lambda^3$ -phospholes are generally too sensitive toward oxygen to be used as material in OLEDs, this compound was derivatized in good yields by *in situ* oxidation into thioxophosphole **3** (^{31}P NMR: $+17.0$ ppm) and oxophosphole **4** (^{31}P NMR: $+11.9$ ppm) (Scheme 1). The corresponding gold complex **5** (^{31}P NMR: -8.0 ppm) was also readily prepared by reacting **2** with $\text{AuCl}(\text{tetrahydrothiophene (tht)})$ (see Scheme 1). These novel air-stable derivatives were purified by column chromatography and fully characterized by multinuclear NMR spectroscopy and high-resolution mass spectrometry (HR-MS).

Scheme 1. Synthetic Routes to Furan–Phosphole Derivatives **2–5**



(3) (a) Salzner, U.; Lagowski, J. B. P.; Pickup, G.; Poirier, R. A. *Synth. Met.* **1998**, *96*, 177. (b) Cyranski, M. K.; Krygowski, T. M.; Katritzky, A. R.; Von Ragué Schleyer, P. J. *Org. Chem.* **2002**, *67*, 1333.

(4) (a) Gidron, O.; Diskin-Posner, Y.; Bendikov, M. *J. Am. Chem. Soc.* **2010**, *132*, 2148. (b) Bunz, U. H. F. *Angew. Chem., Int. Ed.* **2010**, *49*, 5037.

(5) (a) Mitsui, C.; Tsuji, H.; Sato, Y.; Nakamura, E. *Chem.–Asian J.* **2012**, *7*, 1443. (b) Mitsui, C.; Soeda, J.; Miwa, K.; Tsuji, H.; Takeya, J.; Nakamura, E. *J. Am. Chem. Soc.* **2012**, *134*, 5448. (c) Walker, B.; Tamayo, A. B.; Dang, X.-D.; Zalar, P.; Seo, J. H.; Garcia, A.; Tantiwivat, M.; Nguyen, T.-Q. *Adv. Funct. Mater.* **2009**, *19*, 3063. (d) Wu, C.-C.; Hung, W.-Y.; Liu, T.-L.; Zhang, L.-Z.; Luh, T.-Y. *J. Appl. Phys.* **2003**, *93*, 5465. (e) Aleveque, O.; Frere, P.; Leriche, P.; Breton, T.; Cravino, A.; Roncali, J. *J. Mater. Chem.* **2009**, *19*, 3648. (f) Woo, C. H.; Beaujuge, P. M.; Holcombe, T. W.; Lee, O. P.; Fréchet, J. M. J. *J. Am. Chem. Soc.* **2010**, *132*, 15547. (g) Lin, J. T.; Chen, P.-C.; Yen, Y.-S.; Hsu, Y.-C.; Chou, H.-H.; Yeh, M.-C. *P. Org. Lett.* **2008**, *11*, 97.

(6) (a) Hissler, M.; Dyer, P. W.; Réau, R. *Coord. Chem. Rev.* **2003**, *244*, 1. (b) Baumgartner, T.; Réau, R. *Chem. Rev.* **2006**, *106*, 4681.

(7) (a) Bouit, P.-A.; Escande, A.; Szucs, R.; Szieberth, D.; Lescep, C.; Nyulási, L.; Hissler, M.; Réau, R. *J. Am. Chem. Soc.* **2012**, *134*, 6524. (b) Ren, Y.; Kan, W. H.; Henderson, M. A.; Bomben, P. G.; Berlinguette, C. P.; Thangadurai, V.; Baumgartner, T. *J. Am. Chem. Soc.* **2011**, *133*, 17014. (c) Deschamps, E.; Ricard, L.; Mathey, F. *Angew. Chem., Int. Ed. Engl.* **1994**, *33*, 1158. (d) Matano, Y.; Nakashima, M.; Imahori, H. *Angew. Chem., Int. Ed.* **2009**, *48*, 4002. (e) Yavari, K.; Moussa, S.; Ben Hassine, B.; Retaillieu, P.; Voiturez, A.; Marinetti, A. *Angew. Chem., Int. Ed.* **2012**, *51*, 6748. (f) Dienes, Y.; Eggenstein, M.; Kárpáti, T.; Sutherland, T. C.; Nyulási, L.; Baumgartner, T. *Chem.–Eur. J.* **2008**, *14*, 9878. (g) Fukazawa, A.; Hara, M.; Okamoto, T.; Son, E.-C.; Xu, C.; Tamao, K.; Yamaguchi, S. *Org. Lett.* **2008**, *10*, 913. (h) Fukazawa, A.; Yamada, H.; Yamaguchi, S. *Angew. Chem., Int. Ed.* **2008**, *47*, 5582. (i) Weymies, W.; Zaal, M.; Slootweg, J. C.; Ehlers, A. W.; Lammertsma, K. *Inorg. Chem.* **2011**, *50*, 8516.

(8) (a) Chen, H.; Delaunay, W.; Yu, L.; Joly, D.; Wang, Z.; Li, J.; Wang, Z.; Lescep, C.; Tondelier, D.; Geffroy, B.; Duan, Z.; Hissler, M.; Mathey, F.; Réau, R. *Angew. Chem., Int. Ed.* **2012**, *51*, 214. (b) Fave, C.; Cho, T.-Y.; Hissler, M.; Chen, C.-W.; Luh, T.-Y.; Wu, C.-C.; Réau, R. *J. Am. Chem. Soc.* **2003**, *125*, 9254. (c) Joly, D.; Tondelier, D.; Deborde, V.; Delaunay, W.; Thomas, A.; Bhanuprakash, K.; Geffroy, B.; Hissler, M.; Réau, R. *Adv. Funct. Mater.* **2012**, *22*, 567. (d) Ren, Y.; Baumgartner, T. *Dalton Trans.* **2012**, *41*, 7792.

(9) (a) Matano, Y.; Saito, A.; Fujita, M.; Imahori, H. *Heteroatom Chem.* **2011**, *22*, 457. (b) Deschamps, E.; Ricard, L.; Mathey, F. *Heteroatom Chem.* **1991**, *2*, 377. (c) Tran Huy, N. H.; Lu, Y.; Nien Ah Qune, L. F.; Mathey, F. *J. Organomet. Chem.* **2012**, *1016*, jorganchem.2012.08.032.

These results show that the P-center of the mixed furan-phosphole **2** retains the versatile reactivity of phosphole derivatives. It is interesting to note that the ^{13}C NMR chemical shifts of the phosphole rings of furan derivatives **3–5** are markedly different from those of their thiophene analogs of type **C** (Figure 1 and SI), suggesting that the different electronic properties (π -donor ability and electronegativity) of the O and S atoms strongly influence the electronic distribution within the fused frameworks.^{7f}

The structures of **3–5** were determined by X-ray diffraction. Since no solid-state structure of fused heteropentacene gold-complex is known to date, the discussion will focus on this compound. This study confirmed the proposed structure and shows that the conjugated system including the five conjugated rings is fully planar (Figure 2a). As already observed for other Au^{I} -phosphole complexes, the P–Au–Cl fragment is not linear (P–Au–Cl = 173°).^{8b} The phosphorus atom exhibits a distorted tetrahedral geometry with usual P–C bond lengths (1.79 Å). It is interesting to note that the furan rings display a dissymmetric character. The single C–O and double C=C bonds within the PCCO path are quasi-similar (1.36 ± 1 Å) and notably shorter than their benzo-counterpart (1.40 Å). This dissymmetry suggests that the O-atom is effectively conjugated with the P–C=C double bond substituted by an electron-withdrawing σ^3, λ^4 -P moiety (see Table S1, SI). Two features are worth noting. First, this structural molecular feature is observed for all compounds **3–5** (see Figures S4, S5 and Table S1, SI), having similar backbone and withdrawing σ^3, λ^4 -P moieties. Second, this effect is not observed for the corresponding thiophene-thiooxophosphole derivatives **C** (Figure 1) characterized by X-ray diffraction studies,^{7f} showing that the impact of replacing S by O within this planar conjugated platform. Remarkably, complex **5** crystallizes as dimers that are closely packed due to a combination of both π – π interactions (π – π distances, 3.40 Å) and aurophilic interaction ($d_{\text{Au–Au}} = 2.99$ Å) (Figure 2b).¹⁰ Furthermore, these dimers are engaged in intermolecular π – π interactions ($d = 3.55$ Å) resulting in the formation of infinite π -stacked columns (Figure 2c).

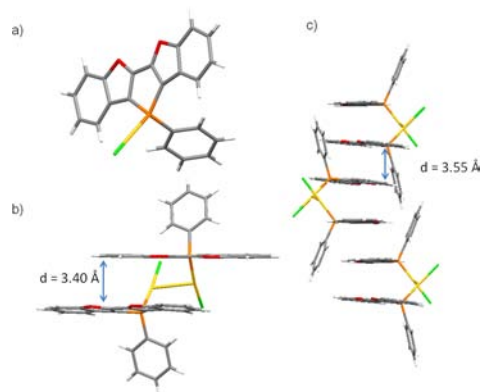


Figure 2. (a) View of crystallographic structure of **5**, (b) view of the dimers and (c) view of the packing along the x axis.

In contrast to what is observed with P,S-monomers **C** (Figure 1), the thiooxo and -oxo-phospholes **3,4** do not organize in the solid state via π – π interactions (see SI). This information is of prime importance for further incorporation of the compounds in OLEDs devices, since intermolecular π – π interactions induce strongly modified solid state emission behavior.¹¹

Optical properties of **3–5** were studied in CH_2Cl_2 by means of UV–vis absorption and fluorescence (Figures 3, S7 (SI) and Table 1). The three compounds show broad absorption in the visible range ($\lambda_{\text{max}} = 380$ nm, see Figure S7, SI) attributed to a π – π^* transition of the conjugated backbone confirmed by density functional theory calculations (DFT) at the B3LYP/6-31+G (d, p) level (Figure 3). The substitution of the P atom only weakly modifies the optical transitions. Compared to their thiophene analogs **C**, **3–5** display slightly blue-shifted transition.^{7f} This observation is also in accordance with the measurements showing a reduced HOMO–LUMO gap in the oligo-thiophene series compared to its oligofuran analog.⁴ The effect of the P-environment is more pronounced on the emission properties of **3–5** (Figure 3). A gradual decrease of the maximal emission wavelength is observed in the series **4–3–5**, as already observed on phosphole oligomers.^{12,8b} P-substitution also affects the fluorescence quantum yield (Table 1). Notably, **4** and **5** display high quantum yield (65–73%), making these derivatives good candidates for use as emitters in light-emitting device. Furthermore, the solid-state emission matches the emission in diluted solution as shown Figure 4 in the case of compound **4**.

Table 1. Photophysical and Electrochemical Data

	λ_{abs}^a [nm]	$\log \epsilon$	λ_{em}^b [nm]	Φ_{F}^c	$E_{\text{ox}}^{\text{ox},d}$ [V]	$E_{\text{red}}^{\text{red},d}$ [V]
3	391	4.4	480	0.03	+1.09	–2.06 ^e
4	390	4.3	491	0.65	+1.20	–2.08 ^e
5	380	4.5	470	0.73	+1.17 ^e	–2.03 ^e

^a In CH_2Cl_2 (10^{-5} M). ^b In CH_2Cl_2 (10^{-5} M) with ($\lambda_{\text{ex}} = 370$ nm). ^c Measured relative to quinine sulfate (H_2SO_4 , 0.1 M), $\phi_{\text{ref}} = 0.546$. ^d In CH_2Cl_2 with $\text{Bu}_4\text{N}^+\text{PF}_6^-$ (0.2 M) at a scan rate of 100 mV s^{-1} . $E_{\text{ox}}^{\text{ox}}$ ($E_{\text{red}}^{\text{red}}$) = $1/2(E_{\text{pc}} + E_{\text{pa}})$ for reversible process, otherwise $E_{\text{ox}}^{\text{ox}} = E_{\text{pa}}$. Potentials vs ferrocene/ferrocenium. ^e Reversible process.

Redox properties of **3–5** were studied by means of cyclic voltammetry (CH_2Cl_2 , 0.2 M Bu_4NPF_6 , $v = 100 \text{ mV s}^{-1}$). All compounds display amphoteric redox character with oxidation and reduction waves at relatively low potentials (Table 1). Typically, **3** displays an irreversible oxidation wave ($E_{\text{ox}}^{\text{ox}} = +1.09$ V vs Fe) and a reversible reduction wave ($E_{\text{red}}^{\text{red}} = -2.06$ V vs Fe). P-substitution has a weak impact on the redox properties, as illustrated by the data presented in Table 1. Compared to its thiophene analog, **3–5** display lower oxidation and reduction potential, with

(10) No proof of formation of these Au–Au interactions in solution was observed

(11) Note that the absence of intramolecular interaction might be detrimental to the charge transport in the device.

(12) Hay, C.; Hissler, M.; Fischmeister, C.; Rault-Berthelot, J.; Toupet, L.; Nyulaszi, L.; Réau, R. *Chem.—Eur. J.* **2001**, *7*, 4222.

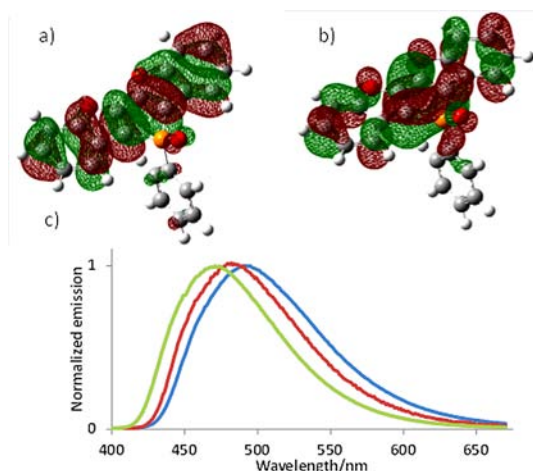


Figure 3. (a) HOMO of **4**, (b) LUMO of **4**, and (c) normalized emission spectra in CH₂Cl₂ of **3** (red), **4** (blue) and **5** (green).

a global increase of the electrochemical gap.^{7f} These data fit with the observed general trend that exchanging sulfur for oxygen in conjugated five-membered oligomers results in changes such as increasing the HOMO–LUMO gap and lowering the oxidation potential.⁴

Since compounds **3–5** are developed as emitters for OLEDs, it was of interest to investigate their thermal stability. The compounds **3** and **4** display decomposition temperature above 250 °C and a melting point at 220 °C indicating good thermal stabilities which is a critical issue for device stability and lifetime. Note that compound **5** is less thermally stable than its analogs **3** and **4** with decomposition temperature of 240 °C.

Taking in account the thermal stabilities and the physical properties of compounds **3–5**, only compound **4** was used as emitting material (EM, pure or doped in a DPVBi matrix) in multilayered OLEDs having a classical structure (indium tin oxide (ITO)/copper phthalocyanine (CuPc) (10 nm)/*N,N'*-diphenyl-*N,N'*-bis(1-naphthylphenyl)-1,1'-biphenyl-4,4'-diamine (α -NPB) (50 nm)/EM (15 nm)/4,4'-bis (2,2'-diphenylvinyl) biphenyl (DPVBi) (35 nm)/bathocuproine (BCP) (10 nm)/tris(8-hydroxyquinolato)aluminum (Alq3) (10 nm)/LiF (1.2 nm) /Al (100 nm) configuration, see Figure S9, SI). In a first device **A**, mixed phosphole-furan **4** was used as pure emitter. In this case, the emission wavelength ($\lambda_{\text{EL}} = 532$ nm) is red-shifted by ca. 40 nm compared to the solid-state photoluminescence of **4** (Figure 4). However, the increase of the current density does not impact the emission wavelength of device **A** (see Figures S10, S12, SI), proving that this emission is not due to degradation of the material. In this device, luminance and external quantum efficiency are moderate (Table 2). It is believed that charge transport in **4** is low, causing this low efficiency. Derivative **4** was then used as dopant in a DPVBi matrix (doping rate 3.6% w, device **B**). In this case, the electroluminescence wavelength which is not affected by the increase of the current density, matches the emission of **4** in the solid state (Figures 4, S13, SI). The emission of DPVBi is

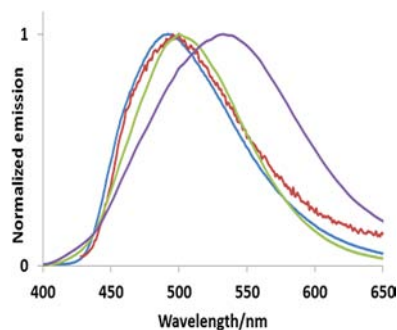


Figure 4. Photoluminescence of **4** in solution (CH₂Cl₂, 10^{−5} M) (blue) and in the solid state (red); electroluminescence of device **B** (green) and device **A** (purple).

Table 2. Electroluminescent Performance of Devices **A** and **B**

device	λ_{EL} [nm]	V_{on}^a [V]	B_{30}^b [cd.cm ^{−2}]	EQE_{30}^b [%]	power efficiency [lm.W ^{−1}] ^b	x^b	y^b
A	532	5.66	175	0.45	0.33	0.32	0.47
B	500	5.70	1248	2.29	1.55	0.22	0.43

^a Measured for $B = 0.1$ cd m^{−2}. ^b Measured at 30 mA cm^{−2}

not observed, indicating a quantitative energy transfer from the DPVBi to the emitter **4**. The external quantum efficiency of the device is close to the one of the DPVBi reference. In this case, the efficacy of the device is not limited by the charge transport of **4**, which explains the better properties of device **B** compared to device **A**.

In conclusion, three novel benzofuran-fused phosphole heteroacenes **3–5** were synthesized and fully characterized. These P,O-containing acenes display distinct properties compared to their S-analogs. The high emission quantum yields of **4** associated with good thermal stability allowed the use of this novel scaffold in OLED emitting in the blue-green region.

Acknowledgment. This research is supported by the Ministère de la Recherche et de l'Enseignement Supérieur, the University of Rennes 1, the CNRS (AIL FOM), IUF. NSFC (No. 21072179) and Henan Science and Technology Department (114300510007) of China. COST CM0802 (Phoscinet) is also acknowledged. The authors are grateful to C. Lescop (CNRS - Université de Rennes 1) for X-ray diffraction studies and to J. Troles (CNRS - Université de Rennes 1) for the DSC measurements.

Supporting Information Available. Synthetic procedure, complete characterizations, X-ray crystallographic data and CIF files for **3–5**, computational details, device preparation. This material is available free of charge via the Internet at <http://pubs.acs.org>.

The authors declare no competing financial interest.